Vietnam Journal of Science and Technology ***60*** *(3) (2022) 350-361*

doi:10.15625/2525-2518/16115

SUSTAINABLE CHEMISTRY OF CHITOSAN ASSEMBLIES PREPARED THROUGH TEMPLATING AND CARBONIZATION

Le Thi Anh Phuong[1, 7], Vu Phi Tuyen[2, *], Nguyen Xuan Ca[3], Thi Le Hoa[4], Phan Van Do[5], Luong Duy Thanh[5], Dang Thi Thanh Nhan[6, *], Nguyen Thanh Dinh[7, *]

[1]*Ba Ria Vung Tau University, 80 Truong Cong Dinh Street, Vung Tau, Viet Nam*

[2]*Center for High Technology Development, 18 Hoang Quoc Viet, Ha Noi, Vietnam*

[3]*Institute of Science and Technology, TNU – University of Sciences, Thai Nguyen, Viet Nam*

[4]*Department of Chemistry, Hue University of Sciences, Hue University, 77 Nguyen Hue, Hue City, Viet Nam*

[5]*Irrigation University, 175 Tay Son, Ha Noi, Viet Nam*

[6]*Department of Chemistry, Hue University of Education, Hue University, 34 Le Loi, Hue, Viet Nam*

[7]*Institute of Applied Material Science, Vietnam Academy of Science and Technology, 1A Thanh Loc 29, Ho Chi Minh City, Viet Nam*

*****Emails: *tuyenvuphi@yahoo.com, nhandang@hueuni.edu.vn, dinhthanhng@yahoo.com.vn*

Received: 23 June 2021; Accepted for publication: 9 August 2021

Abstract. Biomimicry is a fascinating approach to inspire for preparing hierarchical structures of functional materials from nature through templating and transformation methods. In this work, abundantly discarded crab shell was used as a starting material to extract chitosan for investigating its complex self-assembly for material development. Chitosan macromolecules self-assembled in acidic media to form flexible, crack-free, transparent chitosan bioplastic-like membranes after drying. Chitosan bioplastics are further investigated for their physical properties through the chemistry of polymeric cross-linking. Under complexation, chitosan can self-assemble with tetramethylorthosilicate to form silica/chitosan composite membranes. The calcination of the silica/chitosan assemblies under air afforded freestanding mesoporous silica films. Silica materials may be used as a hard template, catalyst support, adsorbent, and in the chromatography. Alternatively, the pyrolysis of the silica/chitosan under nitrogen formed silica/carbon composites. The carbonized composite was etched the silica component away to obtain freestanding mesoporous carbon film supercapacitors. Cyclic voltammogram (CV) technique was used to evaluate electrochemical property of this sustainable chitosan-derived mesoporous carbon film. The obtained CV curves are fairly similar to a leaf-like shape from 2 $mV.s^{-1}$ to 200 $mV.s^{-1}$ with the specific capacitance (Cs) at 2 $mV.s^{-1}$ is 210 $F.g^{-1}$. Our method demonstrates that the thin-film features and hierarchical structure of the parent chitosan can be replicated in the sustainable mesoporous materials of silica and carbon.

Keywords: chitosan, silica, carbon, mesoporosity, templating, carbonization

Classification numbers: 1.1.5, 1.4.2, 2.2.2, 2.4.1, 2.5.2, 2.9.4

1. INTRODUCTION

Biomaterials with hierarchical structures inspired by nature are generally evolved by molecular self-assembly of micro- and nanoscale elements [1]. Biopolymeric self-assembly is a biomimetic pathway to fabricate sustainable materials with hierarchical structures, resembling micro/nanoscale biomaterials found in nature [2]. Surfactant templating was primarily used to construct ordered mesoporous silica materials in the 1990s and later extended to carbon materials and others [3, 4]. Due to the uniqueness of the hierarchical pore textures, the mesoporous silica and carbon materials are useful candidates for applications in catalyst supports, liquid chromatography, adsorbents, optical elements, energy storage and conversion [5 - 7].

Hierarchical structures of polysaccharides are used as a biotemplate and a carbon source to synthesize solid-state materials with remarkable properties via mimicry, replication, and transformation [8, 9]. Chitosan is a deacetylated form of chitin abundantly found in shells of crabs and shrimps, which can be prepared by treating chitin with strong base [10]. Similar to natural chitin, chitosan generally remains complex hierarchical structures and possesses good properties that are valuable for researchers to exploit [11]. Chitosan chemically extracted from crustacean shells is a renewable resource to develop applications in drug delivery, gelling agents, absorbents, and tissue engineering [12]. Remarkably, chitosan is a cationic polymer, which is typically protonated in acid to dissolve into a homogeneous solution. The acidic chitosan solution can self-assemble by either itself or with additives under drying to form functional membranes with hierarchical organization [13]. The chitosan structure can be used as a template for solid-state materials to create hierarchical porous structures with high surface area [14]. Moreover, chitosan is also a renewable carbon source for developing carbon materials for energy storage and conversion application [15]. Upon carbonization and transformation, the hierarchical porous structures of chitosan macromolecules and/or nanofibrils can be conserved in bioinspired carbon materials. The sustainable chemistry of chitosan is fascinating to exploit its complex structure, chemical composition, and membrane self-assembly for innovating advanced functional materials to boost applications. Similar to familiar carbohydrates such as cellulose and alginate, chitin and chitosan have also attracted much attention of research at the academic and industrial scopes to boost their economic values [16]. Over the past decades, extensive studies of different versions of chitin and chitosan have been carried out to develop sustainable materials and applications. For example, chitin solution can be self-assembled for membrane, templated for solid-state materials, and carbonized for hierarchical carbon [17]. Alternatively, chitosan can be turned to a water-soluble form for gels, fibrils and membranes or can even undergo liquid transfer carbonization to break down to luminescent carbon nanorods [18]. However, there seems to be a lack of focus on exploiting the function of chitosan as simultaneous template and carbon source for silica and carbon.

Herein, we reported the use of chitosan as a biotemplate and a carbon source to fabricate hierarchical mesoporous silica and carbon from silica/chitosan assemblies. Chitosan chemically extracted from crab shells was dissolved in acidic media to condense with silica to form silica/chitosan composite membranes during evaporation-induced self-assembly. The composites were heated under air to remove the chitosan template in order to generate transparent hierarchical mesoporous silica membranes. The composites were carbonized in nitrogen atmosphere and treated with hot alkali to etch silica away, and hierarchical mesoporous carbon membranes with supercapacitance performance were finally obtained.

2. EXPERIMENTAL SECTION

2.1. Chemicals

Discarded shells of cooked crabs (*Scylla olivacea*) were collected from local seafood restaurants. These shells were cleaned by washing with copious water and dried at room temperature for material preparation. Tetramethylorthosilicate (≥ 99%) was purchased from Sigma-Aldrich. Other chemicals such as acetic acid, sodium hydroxide, sulfonic acid, and ethanol were received from standard suppliers. The chemicals were used without further purification.

2.2. Preparation of chitosan solution

Cleaned crab shells (~12 g) were treated with $NaOH_{(aq)}$ (250 mL, 5 wt%) at 90 °C for 6 h to remove protein and then treated with $HCl_{(aq)}$ (250 mL, 0.1 M) at room temperature for 24 h to dissolve calcium carbonate. The resulting shells were bleached with a hot H_2O_2 solution to oxidize organic pigments and generated chitin. Purified chitin shells (~3.5 g) obtained after washing thoroughly with water were soaked in $NaOH_{(aq)}$ (500 mL, 50 wt%) and heated at 90 °C for 8 h for deacetylation. The deacetylation was repeatedly performed for three times to increase the dissolution of chitosan in acetic acid solution. The fully deacetylated product was washed thoroughly with water to obtain chitosan. The resulting chitosan sample was dissolved in 2% acetic acid under stirring to form an acidic chitosan solution with transparent homogeneity.

2.3. Preparation of chitosan bioplastic-like membranes

30 mL of the chitosan solution (4.0 wt%, pH ~ 2) was poured to a 150 mm-sized polystyrene Petri dish and evaporated at room temperature to form a crack-free, flexible chitosan membrane after 3 days. The dried membrane formed from chitosan assemblies was soaked in ethanol for 30 min to remove adsorbed water by solvent exchange, forming a tough chitosan bioplastic-like membrane.

2.4. Preparation of hierarchical mesoporous silica and carbon films

Tetramethylorthosilicate (620 mg) was mixed with 10 mL of the chitosan solution (4.0 wt.%, pH ~ 2) at a silica/chitosan weight ratio of 40:60 wt.% under stirring at room temperature for 30 min to form a silica/chitosan mixture. The mixed solution was poured to a 60 mm-sized polystyrene Petri dish and dried at room temperature to form a crack-free silica/chitosan composite membrane after 3 days. The silica/chitosan composite membrane (~ 600 mg) was calcined under air at 550 ^{o}C in an oven at a heating rate of 5 ^{o}C min^{-1} for 5 h to form ~ 110 mg of transparent mesoporous silica films. Alternatively, the silica/chitosan composites (~ 500 mg) were carbonized under nitrogen at 800 ^{o}C in a tube furnace at a heating rate of 5 ^{o}C min^{-1} for 5 h to generate ~ 70 mg of black mesoporous carbon films.

2.5. Structural characterization

Powder X-ray diffraction (PXRD) pattern of the sample was recorded on an Advance Bruker D8 X-ray diffractometer, using Cu Kα radiation (λ = 1.5418 Å). Raman spectrum was recorded on a Micro Raman LabRAM-1B spectrometer with 785 nm excitation. Scanning electron microscope (SEM) images of the samples were obtained on a Hitachi S4700 electron microscope. Small pieces of broken membranes and films were placed on aluminum stubs and then coated with Au for silica and Au-Pd for carbon. Polarized optical microscopy (POM) was performed between crossed polarizers on an Olympus BX40 microscope. Transmission electron microscope (TEM) images of the samples were obtained on a JEOL- JEM 1010 microscopy. The film samples were gently crushed to form powders and then suspended in ethanol and later

dropped on TEM copper grids for TEM preparation. It was noted that chitosan/silica composite samples typically burned faster in an oven by air calcination than in a TGA chamber. Thermogravimetric analysis (TGA) of the samples (~10 mg) were conducted at a heating rate of 10 °C.min^{-1} under air and/or nitrogen atmosphere from RT to 800 °C using a Labsys TG/DSCSE-TARAM thermogravimetric analyzer. Fourier transform infrared absorption spectrum (FTIR) was recorded on a PERKIN ELMER FT-IR Spectrometer with the KBr pellet technique. Nitrogen adsorption-desorption isotherms (US) were obtained using a Micromeritics at 77 K and the carbon film samples (~120 mg) were degassed at 150 ˚C in vacuum for 4 h before measurements. Cyclic voltammetry measurements were performed with a two-electrode configuration using a Brinkmann PGSTAT12 Autolabpotentiostat. The freestanding carbon films were weighed and soaked in a 1 M H_2SO_4 aqueous solution for at least 24 h. Two pieces of symmetrical carbon films, each piece of 110 mm-sized round Whatman filter paper, and 1 M H_2SO_4 were used as electrodes, separator, and electrolyte, respectively. Stainless-steel collectors sandwiched two fibers with a filter paper separator, and they were placed in a Swagelok two-electrode cell.

3. RESULTS AND DISCUSSION

3.1 Chitosan membranes

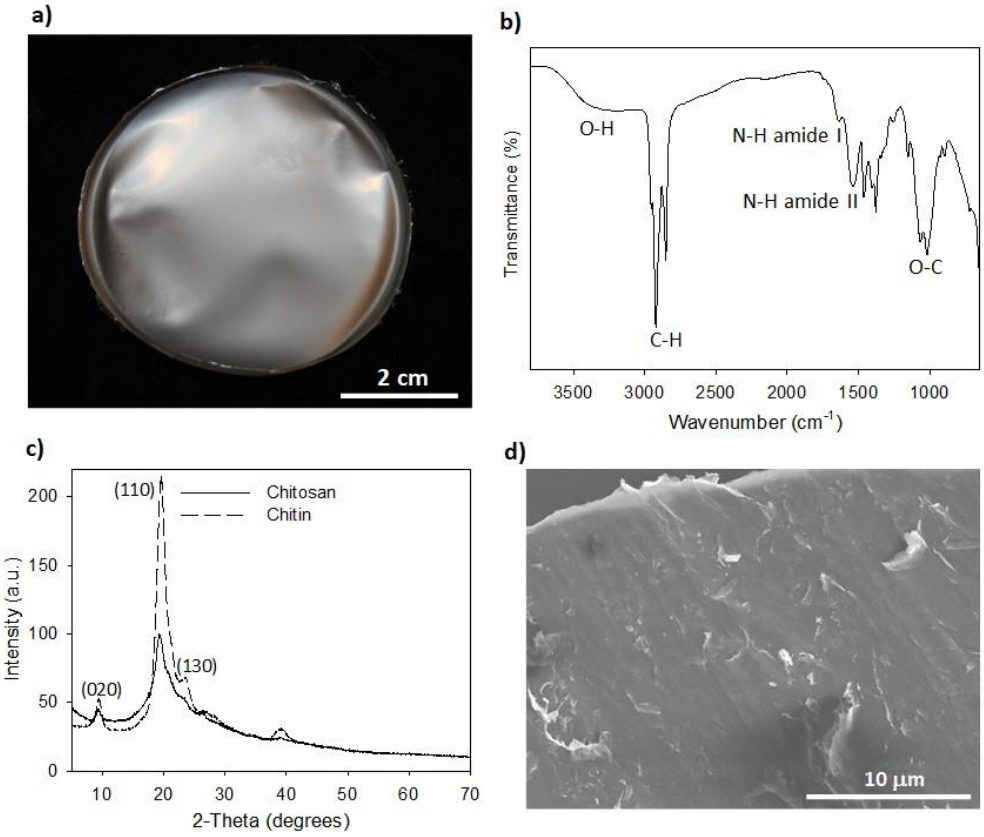

Figure 1. Self-assembly of acidic chitosan macromolecules into chitosan bioplastic-like membrane. a) Photo of flexible, large, crack-free chitosan membrane derived from the self-assembly of acidic chitosan solution prepared from crab shells. b) IR spectra of chitosan, c) PXRD patterns of chitin and chitosan, and d) SEM image of chitosan membrane.

Chitosan was prepared by treating chitin purified from the cleaned crab shells with a 50 % NaOH solution at 90 ^{o}C for 8 h. The resulting chitosan was dissolved in 2 % acetic acid to form a homogeneous acidic chitosan solution. A desired volume of the chitosan solution can be casted on a substrate (*e.g.*, polystyrene Petri dish) under air drying for at least 3 days to yield a freestanding chitosan membrane (Figure 1a). The dried chitosan membranes are transparent, flexible, crack-free, and have their diameter up to a few tens of centimeters, depending on the volume of the solution employed. Infrared (IR) spectrum (Figure 1b) of the prepared chitosan membrane shows a hydroxyl stretch at 3480 cm^{-1}, amide stretches at 1560 - 1660 cm^{-1}, and a C-O-C stretch at 1030 cm^{-1}, which are characteristic of chitin molecules [19]. Powder X-ray diffraction (PXRD) patterns (Figure 1c) of the purified chitin show sharp diffraction peaks at 9.5^{o}, 19^{o}, 23^{o} 2θ corresponding to the (020), (110), (130) planes, which are characteristic of α-chitin crystallites [20].

After deacetylation, the chitosan still remains the main diffraction peaks, but strongly decreases their intensity, indicating that the chitosan has considerably lower crystallinity than chitin. SEM image (Figure 1d) shows homogeneously packed structure with less nanofibril-like textures in the chitosan membranes. This also proves the polymeric regeneration of chitosan macromolecules into hierarchically layered membranes by self-assembly.

3.2. Chitosan/silica composite membranes

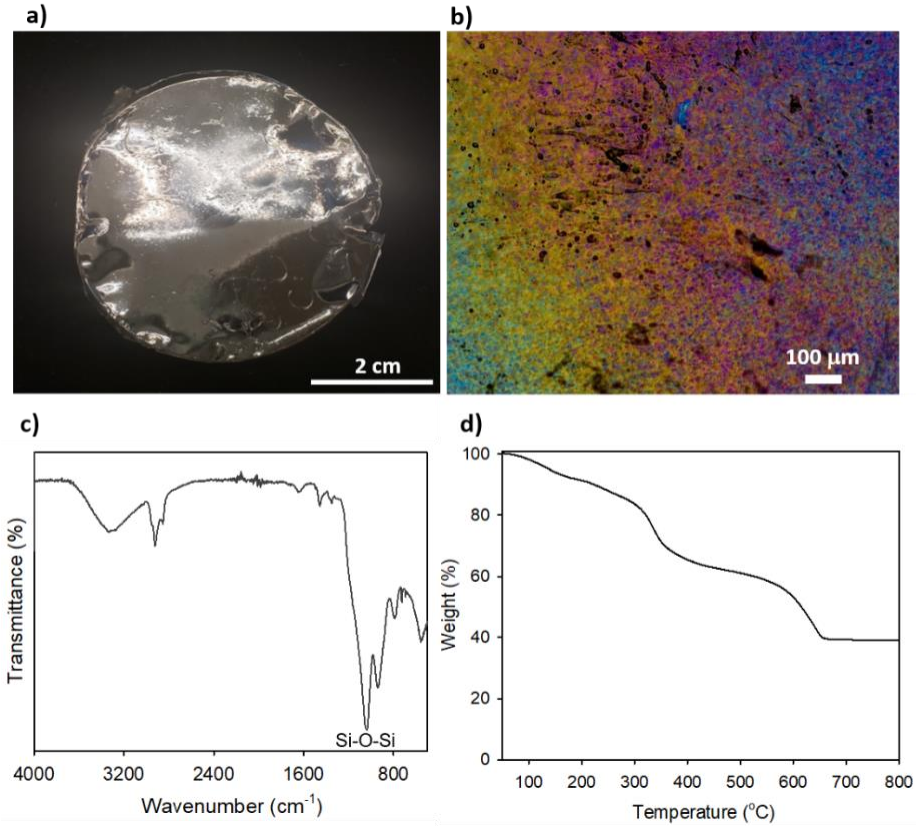

Figure 2. Evaporation-induced self-assembly of tetramethylorthosilicate with acidic chitosan into silica/chitosan composite membranes. a, b) Photo of assembled silica/chitosan composite membrane, c) IR of silica/chitosan, d) TGA curve of silica/chitosan composites running at 10 ^{o}C.min^{-1} under air atmosphere, and POM image of silica/chitosan composite membrane.

To demonstrate the role of chitosan as both a template and a carbon precursor in materials chemistry, self-condensation of an acidic chitosan solution with tetramethylorthosilicate into composite membranes was performed. These composites can be used as a new precursor to innovate functional materials. Typically, we mixed 620 mg of tetramethylorthosilicate with 10 mL of chitosan solution (4 wt%, pH ~ 2) under stirring. In acidic media, tetramethylorthosilicate hydrolyzed to silica condensing onto chitosan macromolecules, forming a homogeneous silica/chitosan mixture. The mixture was poured onto a 60 mm-sized polystyrene Petri dish and allowed to dry at room temperature for at least 3 days to form a large, crack-free silica/chitosan composite membrane (Figure 2a).

The morphological and structural characterizations of the silica/chitosan composites were shown in Figure 2. The silica/chitosan composite membrane shows birefringent colors under polarized optical microscopy (POM), indicating that the chitosan structure is a linear polymer even in the presence of the silica precursor (Figure 2b) [21]. These structural features reflect the natural integrity of the inorganic-organic homogeneity in the silica/chitosan composite assemblies. The IR spectrum (Figure 2c) of the silica/chitosan composite shows IR bands associated with vibrational modes of chitosan and silica, demonstrating the sol-gel condensation between silica and chitosan components.

3.3. Silica films

The chitosan template in the silica/chitosan composites was burned away by heating the sample at 550 ^{o}C under air to recover mesoporous silica films (Figure 3a). The calcined silica films appear highly transparent and thinner than the composite membranes because of the thermal shrinkage under release of the chitosan template. The hierarchical structure of the calcined silica films can be observed in SEM. The top view shows relatively smooth surface and fractural cross sections show a layered structure made of silica micro/nanoparticles aggregates (Figure 3b,c,d). During templation of the mesoporous silica with chitosan polymer, the hierarchical organization of the chitosan template was transferred to the silica at the nanoscale level and the layered structure was imprinted into the calcined silica films during calcination. Thermogravimetric analysis (TGA) of the silica/chitosan composite showed the weight loss of the chitosan component to be ~60 wt.% at 100-500 ^{o}C and left behind ~40 wt.% silica (Figure 2d). PXRD of the calcined silica obtained after chitosan removal shows a broad peak at $2\theta \approx 23^{\circ}$ characteristic of amorphous silica (Figure 4b) [22]. These results prove that the calcination of the composites fully released the chitosan template to recover the pure amorphous silica films. Nitrogen adsorption-desorption isotherms were used to determine the porosity of the calcined silica films. Figure 4c shows that the silica reveals a typical type-IV isotherm with a hysteretic loop in the range of 0.6-1.0P/P_o indicative of mesoporous structure in the calcined films with a Brunauer-Emmett-Teller (BET) surface area of 280 $m^2.g^{-1}$ [23]. The nanosized pores are the gaps between silica particle aggregates and nanosize spaces left behind by chitosan release. TEM images (Figure 4a) of the silica films further show mesoporous networks made of silica particles interconnected with each other within the films. The combination of hierarchical mesochannels and thin-film features into a sustainable, freestanding glass endow with functions of applications in hard templating, catalyst supports, adsorbents, and liquid chromatography [24, 25].

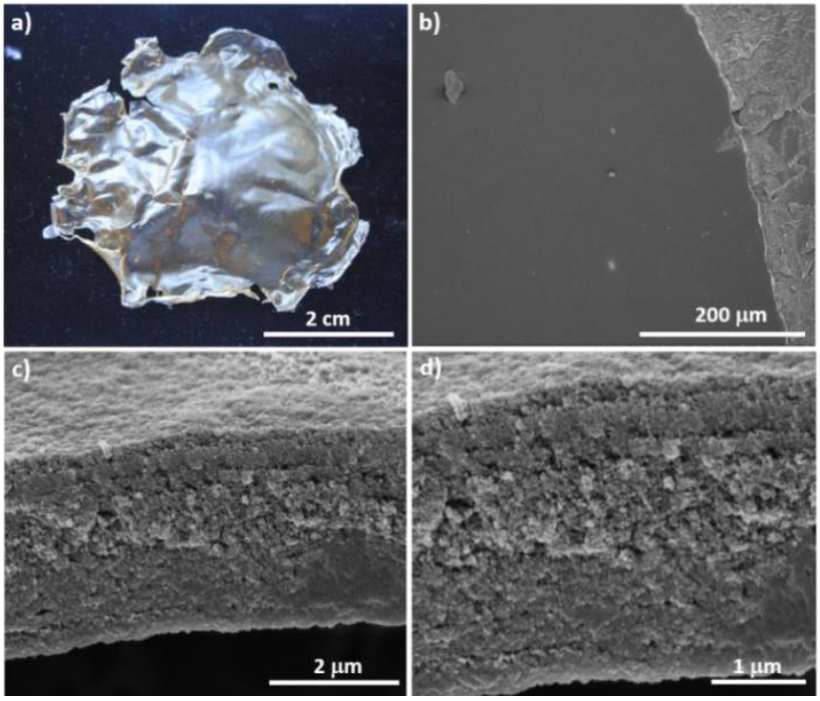

Figure 3. Hierarchical mesoporous silica films obtained after the release of chitosan template by calcination. a) Photo of hierarchical mesoporous silica films with freestanding feature and b,c,d) SEM images of hierarchical mesoporous structure of silica film.

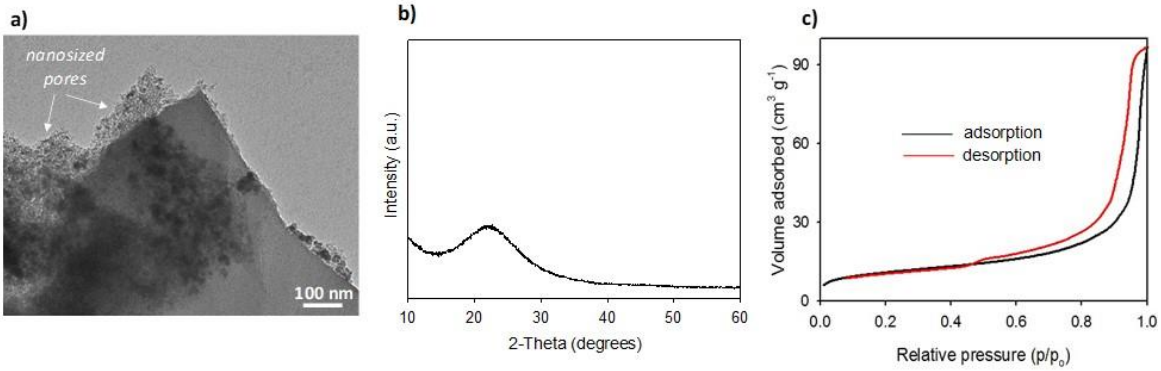

Figure 4. Structural analysis of calcined silica films. a) TEM image of silica, b) PXRD pattern of silica, and c) Nitrogen adsorption-desorption isotherms of mesoporous silica films.

3.4. Carbon films

The carbonization of the silica/chitosan composites was performed by heating the sample under nitrogen at 800 ^{o}C for 7 h to generate black silica/chitosan composite films. The carbonized composites were treated with a hot dilute NaOH solution to dissolve the silica component, thus yielding mesoporous carbon films. The silica/carbon composites appear black in color and volume shrinkage with the similar shape as the silica/chitosan membranes (Figure 5a). The carbonization yield of the chitosan-to-carbon conversion determined by TGA analysis was ~ 20 %. The silica component in the carbonized composites was etched away to obtain the

pure carbon films, which can be confirmed by TGA (Figure 6c). TGA of the pure carbon films shows the near complete burn of carbon occurring at 400 ^{o}C - 600 ^{o}C in air atmosphere.

PXRD pattern of the carbon sample shows two broad peaks at 23^{o} and 43^{o} attributed to amorphous carbon (Figure 6a) [26]. Raman spectra of the pure carbon shows D band at 1350 cm^{-1} (D band) and G band 1580 cm^{-1} corresponding to an amorphous carbon structure (Figure 6b) [27]. These analyses lead to a conclusion that the carbonization of chitosan under the identical experiment yielded the amorphous carbon materials. The porosity of the carbon materials was studied using nitrogen adsorption/desorption isotherms. Figure 6d shows the carbon films having a type-IV isotherm with type-H2 hysteresis loop characteristic of mesoporous structure with a BET surface area of 520 $m^2.g^{-1}$. The nanosized porous networks can also be observed by TEM in Figure 5d. The hierarchical structure of the mesoporous carbon materials can be observed by SEM to show a layered structure of interconnected anisotropic nanoparticles (Figure 5b,c). These morphological features are consistent with the original shape of the parent chitosan in the assembled composites before carbonization and silica etching.

3.5. Supercapacitor performance of carbon films

We used the sustainable chitosan-derived mesoporous carbon film as a freestanding supercapacitor with no binder required to evaluate its electrochemical property by cyclic voltammogram (CV) technique. Two pieces of the mesoporous carbon film electrodes were constructed in symmetrical cells with 1 M H_2SO_4 electrolyte. The electrochemical performance of the mesoporous carbon electrode over a broad range of the scan rates is shown in Figure 6e. The mesoporous carbon electrode exhibits CV curves fairly remaining a leaf-like shape from 2 $mV.s^{-1}$ to 200 $mV.s^{-1}$. The specific capacitance (C_s) of the mesoporous carbon calculated from the CV charge curve at 2 $mV.s^{-1}$ is 210 $F.g^{-1}$, which is comparable with previously reported sustainable carbon supercapacitors [28 - 30].

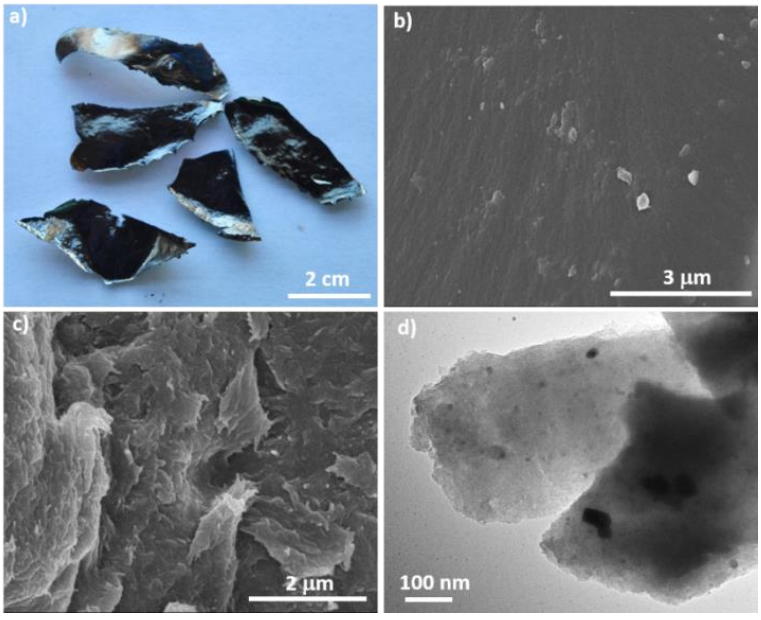

Figure 5. Hierarchical mesoporous silica films derived from chitosan. a) Photo of freestanding hierarchical mesoporous carbon film, b,c) SEM images of carbon film, and d) TEM image of carbon film.

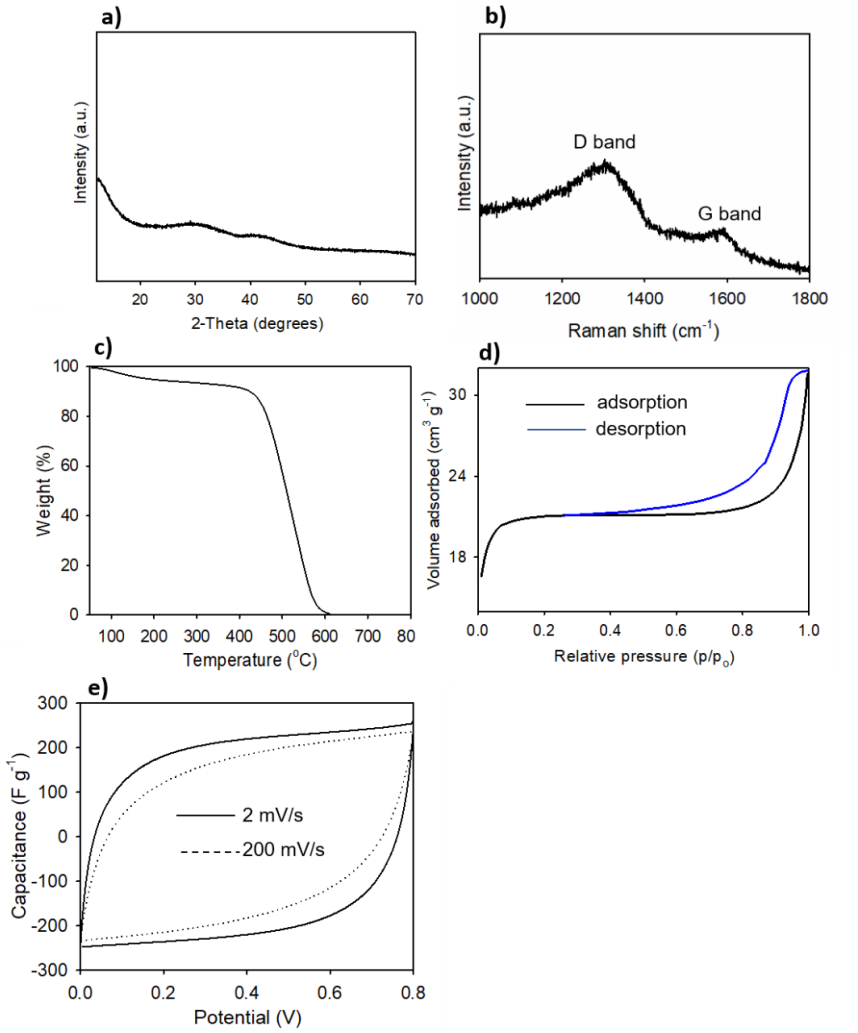

Figure 6. Structural analysis of chitosan-derived mesoporous carbon films. a) PXRD pattern of carbon, b) Raman spectrum of carbon, c) TGA curve of carbon running at a heating rate of 10 ^{o}C min under nitrogen atmosphere, d) Nitrogen adsorption-desorption isotherms, and e) CV curves of mesoporous carbon films in 1 M H_2SO_4 electrolyte at 2 mV.s^{-1} and 200 mV.s^{-1}.

4. CONCLUSIONS

Crab shell-induced chitosan has been used as both biotemplate and carbon precursor to fabricate hierarchical mesoporous structures of silica and carbon with freestanding thin-film features through evaporation-induced self-assembly. The chitosan macromolecules in the acidic solution can self-assemble by themselves to generate flexible, crack-free, transparent chitosan bioplastic-like membranes. Electron microscopy analyses show that the freestanding membranes have a layered structure from the chitosan assemblies. The large chitosan membranes could be used as bioplastics for food packaging and biomedical engineering. The chitosan bioplastics may be more useful for sustainable applications by further investigating to enhance their physical properties through chemistry of polymeric crosslinking. Beyond simplicity, tetramethylorthosilicate was condensed onto chitosan in acidic media to cast into silica/chitosan composite membranes by evaporation-induced self-assembly. We used the silica/chitosan

assemblies as a precursor to develop functional materials. Mesoporous silica films were obtained by thermally removing the chitosan template in the assembled composites. With advances in the structural hierarchy and freestanding film, silica materials may be useful for hard templating, catalyst supports, adsorbents, and chromatography. The silica/chitosan assemblies were carbonized into silica/carbon composites followed by alkali etching to selectively remove silica components to yield mesoporous carbon supercapacitors. Possessing the integrity of the semiconducting property, sustainable carbon materials have great potential for developing energy storage materials. Electron microscopy analyses reveal that the thin-film features and hierarchical layered structure of the parent chitosan are replicated in the prepared materials of the sustainable mesoporous silica and carbon.

***Acknowledgements*:** This research is funded by Vietnam National Foundation for Science and Technology Development (NAFOSTED) under grant number 103.02-2018.365.

CRediT authorship contribution statement: Le Thi Anh Phuong: Conceptualization, Methodology, Software. Vu Phi Tuyen: Data curation, Writing- Original draft preparation. Nguyen Xuan Ca: Visualization, Investigation. Thi Le Hoa: Visualization, Investigation, Phan Van Do: Software, Validation, Luong Duy Thanh: Visualization, Investigation, Dang Thi Thanh Nhan: Writing- Reviewing and Editing. Nguyen Thanh Dinh: Supervision.

Declaration of competing interest: The authors declare that there is no conflict of interest regarding the publication of this article

REFERENCES

1. Zhang C., Mcadams II D. A., and J. C. Grunlan - Nano/Micro-Manufacturing of Bioinspired Materials: a Review of Methods to Mimic Natural Structures, Advanced Materials **28** (30) (2016) 6292-6321. https://doi.org/10.1002/adma.201505555
2. Ikkala O. and G. ten Brinke - Functional Materials Based on Self-Assembly of Polymeric Supramolecules, Science **295** (5564) (2002) 2407-2409.

   https://doi.org/10.1126/science.1067794
3. Kresge C. T., *et al.* - Ordered mesoporous molecular sieves synthesized by a liquid-crystal template mechanism, Nature **359** (6397) (1992) 710-712.

   https://doi.org/10.1038/359710a0
4. Hsueh H. Y., Yao C. T., and Ho R. M. - Well-ordered nanohybrids and nanoporous materials from gyroid block copolymer templates, Chemical Society Reviews **44** (7) (2015) 1974-2018. https://doi.org/10.1039/C4CS00424H
5. Slowing I. I., *et al.* - Mesoporous silica nanoparticles: structural design and applications, Journal of Materials Chemistry **20** (37) (2010) 7924-7937

   https://doi.org/10.1039/C0JM00554A
6. Giraldo L. F., *et al.* - Mesoporous Silica Applications, Macromolecular Symposia **258** (1) (2007) 129-141. https://doi.org/10.1002/masy.200751215
7. Eftekhari A. and Fan Z. - Ordered mesoporous carbon and its applications for electrochemical energy storage and conversion, Materials Chemistry Frontiers **1** (6) (2017) 1001-1027. https://doi.org/10.1039/C6QM00298F

8. Zollfrank C., *et al.* - Biotemplating of inorganic functional materials from polysaccharides, Bioinspired, Biomimetic and Nanobiomaterials **1** (1) (2012) 13-25. https://doi.org/10.1680/bbn.11.00002
9. Yang H., *et al.* - Biomass-Derived Porous Carbon Materials for Supercapacitor, Frontiers of Chemistry **7** (274) (2019). https://doi.org/10.3389/fchem.2019.00274
10. Wang H., J. Qian, and F. Ding - Recent advances in engineered chitosan-based nanogels for biomedical applications, Journal of Materials Chemistry B **5** (34) (2017) 6986-7007. https://doi.org/10.1039/C7TB01624G
11. Meng Q., Heuzey M. C., and Carreau P. J. - Hierarchical Structure and Physicochemical Properties of Plasticized Chitosan, Biomacromolecules **15** (4) (2014) 1216-1224; https://doi.org/10.1021/bm401792u
12. Sousa, M.P., et al., *Bioinspired multilayer membranes as potential adhesive patches for skin wound healing.* Biomaterials Science, 2018. 6(7): p. 1962-1975; Available from: https://doi.org/10.1039/C8BM00319J
13. Cui L., *et al.* - Preparation and characterization of chitosan membranes, RSC Advances **8** (50) (2018) 28433-28439. https://doi.org/10.1039/C8RA05526B
14. Kadib A. E., *et al*. - Chitosan templated synthesis of porous metal oxide microspheres with filamentary nanostructures, Microporous and Mesoporous Materials **142** (1) (2011) 301-307. https://doi.org/10.1016/j.micromeso.2010.12.012
15. Lin Z., *et al.* - Facile synthesis of chitosan-based carbon with rich porous structure for supercapacitor with enhanced electrochemical performance, Journal of Electroanalytical Chemistry **823** (2018) 563-572. https://doi.org/10.1016/j.jelechem.2018.06.031
16. Grishkewich N., Mohammed N., Tang J., Tam K. C. - Recent advances in the application of cellulose nanocrystals, Current Opinion in Colloid & Interface Science **29** (2017) 32-45. https://doi.org/10.1016/j.cocis.2017.01.005
17. Nguyen H. L., *et al*. - The Renewable and Sustainable Conversion of Chitin into a Chiral Nitrogen-Doped Carbon-Sheath Nanofiber for Enantioselective Adsorption, Chem. Sus. Chem. **12** (14) (2019) 3236. https://doi.org/10.1002/cssc.201901176
18. Chau T. T. L., *et al*. - Sustainable carbon-based nanostructures with optoelectronic performance inspired by crustacean shells towards biomimetic pyrolysis and hydrothermal liquid crystal transfer, Optical Materials **116** (2021) 111100.
https://doi.org/10.1016/j.optmat.2021.111100
19. Dimzon I. K. D. and Knepper T. P. - Degree of deacetylation of chitosan by infrared spectroscopy and partial least squares, International Journal of Biological Macromolecules **72 (**2015) 939-945. https://doi.org/10.1016/j.ijbiomac.2014.09.050
20. Goodrich J. D. and Winter W. T. - α-Chitin Nanocrystals Prepared from Shrimp Shells and Their Specific Surface Area Measurement, Biomacromolecules **8** (1) (2007) 252-257. https://doi.org/10.1021/bm0603589
21. João C. F. C., *et al.* - Bio-inspired production of chitosan/chitin films from liquid crystalline suspensions, Carbohydrate Polymers **155** (2017) 372-381.
https://doi.org/10.1016/j.carbpol.2016.08.039
22. Xue S. H., *et al*. - Induced transformation of amorphous silica to cristobalite on bacterial surfaces, RSC Advances **5** (88) (2015) 71844-71848.

https://doi.org/10.1039/C5RA13619A

23. Kruk M., Jaroniec M., and Sayari A. - Adsorption Study of Surface and Structural Properties of MCM-41 Materials of Different Pore Sizes, The Journal of Physical Chemistry B **101** (4) (1997) 583-589. https://doi.org/10.1021/jp962000k
24. Zhang L., *et al.* - Templated Growth of Crystalline Mesoporous Materials: From Soft/Hard Templates to Colloidal Templates, Frontiers of Chemistry **7** (22) (2019). https://doi.org/10.3389/fchem.2019.00022
25. Cecilia J. A., Moreno Tost R., and Retuerto Millán M. - Mesoporous Materials: From Synthesis to Applications, International Journal of Molecular Sciences **20** (13) (2019) 3213. https://doi.org/10.3390/ijms20133213
26. Qiu T., *et al*. - The preparation of synthetic graphite materials with hierarchical pores from lignite by one-step impregnation and their characterization as dye absorbents, RSC Advances **9** (22) (2019) 12737-12746. https://doi.org/10.1039/C9RA00343F
27. Wang Q., Allred D. D., and Knight L. V. - Deconvolution of the Raman spectrum of amorphous carbon, Journal of Raman Spectroscopy **26** (12) (1995) 1039-1043. https://doi.org/10.1002/jrs.1250261204
28. Wang Y., *et al*. - Biomass derived carbon as binder-free electrode materials for supercapacitors, Carbon **155** (2019) 706-726.

    https://doi.org/10.1016/j.carbon.2019.09.018
29. Ghosh S., *et al.* - Natural biomass derived hard carbon and activated carbons as electrochemical supercapacitor electrodes, Scientific Reports **9** (1) (2019) 16315. https://doi.org/10.1038/s41598-019-52006-x
30. Lu H. and Zhao X. S. - Biomass-derived carbon electrode materials for supercapacitors, Sustainable Energy & Fuels **1** (6) (2017) 1265-1281. https://doi.org/10.1039/C7SE00099E